Landau quantization in twisted bilayer graphene: The Dirac comb

M. Kindermann and E. J. Mele

Phys. Rev. B **84**, 161406 — Published 19 October 2011

DOI: 10.1103/PhysRevB.84.161406

Landau Quantization in Twisted Bilayer Graphenes: the Dirac Comb

M. Kindermann[1] and E.J. Mele[2*]
[1] *School of Physics Georgia Institute of Technology Atlanta, GA 30332*
[2] *Department of Physics and Astronomy University of Pennsylvania Philadelphia PA 19104*

We study the Landau quantization of the electronic spectrum for graphene bilayers that are rotationally faulted to produce periodic superlattices. Commensurate twisted bilayers exist in two families distinguished by their sublattice exchange parity. We show that these two families exhibit distinct Landau quantized spectra distinguished both by the interlayer coupling of their zero modes and by an amplitude modulation of their spectra at energies above their low energy interlayer coherence scales. These modulations can provide a powerful experimental probe of the magnitude of a weak coherence splitting in a bilayer and its low energy mass structure.

PACS numbers: 73.22.Pr, 77.55.Px, 73.21.-b,71.70.Di

The massless Dirac model for the low energy electronic physics of single layer graphene is generally preempted by the interlayer motion of the charge carriers in few layer graphenes (FLG's) [1]. In Bernal (AB) stacked bilayer graphenes the interlayer coherence scale is ~ 0.2 eV and the low energy electronic physics [2–5] is readily distinguishable from that of a single layer [6, 7]. Surprisingly, one finds only relatively weak (if any) effects of coherent interlayer motion in rotationally faulted (twisted) FLG's where the symmetry axes in neighboring layers are misaligned by angles $\theta \neq n\pi/3$ [8–13]. Theory suggests that the interlayer coupling scale is reduced in these structures [9, 14–17] but its description poses a rich commensuration problem that can depend on both the rotation angle and the atomic registry of neighboring layers [18, 19]. It is important to understand how this coupling manifests itself in the electronic behavior, distinguishing twisted FLG from both single layer and Bernal bilayer graphene.

In this Letter we show that even weak interlayer coupling in these systems leaves a striking fingerprint on their Landau level (LL) spectra. The coherence splitting produces an interference pattern in the LL spectra observable as an amplitude modulation: the "Dirac comb." The modulation period can greatly exceed the underlying (presumably small) coupling scale and its phase depends on the low energy mass structure. Observation of these modulations through spectroscopy or transport quantifies the coherence between weakly coupled layers.

Landau quantization of a twisted bilayer is studied using a long wavelength theory that includes the effects of lattice commensurability [18]. We study commensurate rotational faults where eclipsed A-sublattice sites are fixed at the origin of the AA stacked stucture and one layer is rotated through angle θ to form a new periodic superlattice. Commensurate rotations can be classified according to their sublattice parity: sublattice even (SE) structures are invariant under exchange of sublattice labels A and B while sublattice odd (SO) structures break sublattice symmetry. In this notation AA stacking (all sites in neighboring layers eclipsed) has $\theta = 0$ (SE), Bernal AB stacking has $\theta = \pi/3$ (SO). The sublattice parity of *any* commensurate rotated structure determines the allowed momentum-conserving interlayer terms in its low energy Hamiltonian [18]. Each layer has Dirac cones in two valleys centered at the K and K' points described by the (unrotated) long wavelength Hamiltonians [20]

$$H_K = -i\hbar v_F \sigma \cdot \nabla;\ H_{K'} = \sigma_y H_K \sigma_y, \tag{1}$$

where the 2×2 σ matrices act on the sublattice (pseudospin) degrees of freedom. For SE structures the interlayer coupling is valley preserving, described by the interlayer operator

$$H_{\rm int}^{\rm SE} = \mathcal{V} e^{i\vartheta} \exp\left(i\varphi \sigma_z \tau_z\right), \tag{2}$$

with 2×2 τ matrices that act on the valley indices. For SO structures the coupling is both interlayer *and* intervalley and has the form

$$H_{\rm int}^{\rm SO} = \frac{\mathcal{V}}{2} e^{i\vartheta} \left(1 + \sigma_z\right) \tau_x \tag{3}$$

(or its valley reversed partner $\sigma_x H_{\rm int}^{\rm SO} \sigma_x$). The coupling strength $\mathcal{V}$ and phase angle φ are determined by the details of the microscopic Hamiltonian while the overall phase ϑ can be removed by a $U(1)$ gauge transformation. In Eqn. (2) φ is not determined geometrically but instead results from the interference of scattering amplitudes at momenta that span the momentum mismatches between Dirac cones of the two layers [18].

The band structures for these two families are shown in the inset of Figure 1. SO bilayers have a pair of bands gapped by the interlayer coupling and a contact point between two quadratically dispersing bands, analogous to the situation for Bernal stacked bilayers except for their θ-dependent interlayer coherence scale $\mathcal{V}$ which can be significantly reduced. SE bilayers feature a *pair* of Dirac nodes at $q = 0$ with equal weights on the two layers offset in energy by the interlayer interaction. Note that the SE bilayers are generically *gapped* (their band extrema occur on a ring in reciprocal space) because of a

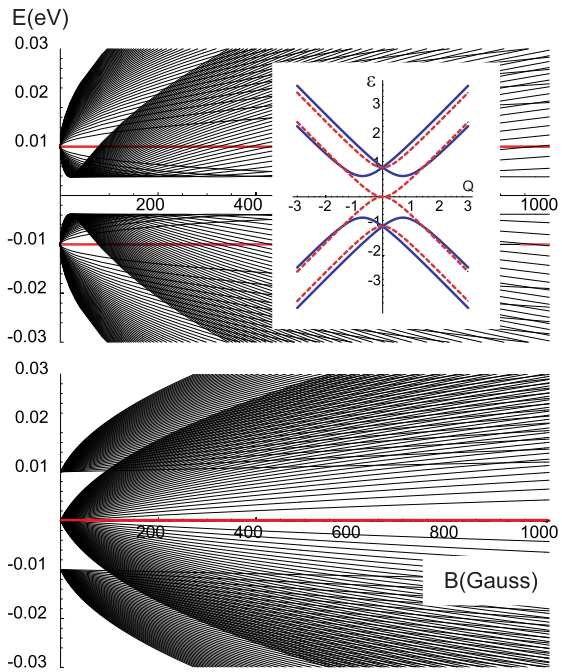

FIG. 1: Inset: Dispersion of the coherence-split low energy bands for commensurate twisted graphene bilayers that are even (blue, solid) and odd (red, dashed) under sublattice exchange. The plot gives the dimensionless energy $\varepsilon = E/\mathcal{V}$ as a function of the scaled momentum $Q = \hbar v_F q/\mathcal{V}$ where $\mathcal{V}$ is the interlayer coherence scale and the pseudospin rotation parameter $\varphi = \pi/4$ for the SE structure. Main figure: Landau level spectra Eqns. (9) and (10) for twisted bilayers for SE and SO families as a function of the field strength with coherence scale $\mathcal{V} = 10\,\text{meV}$. The red lines are states spanned by the zero modes of the two layers.

low energy avoided band crossing. The size of this gap is determined by the pseudospin rotation angle φ in Eqn. (2) and vanishes for the special case of AA stacking where $\varphi = 0$ by symmetry [18].

To study this system in a perpendicular magnetic field $\vec{B}$ we introduce a vector potential in the symmetric gauge $\vec{A} = (\vec{B} \times \vec{r})/2$. Defining $z = (x + iy)/\ell_B$ with magnetic length $\ell_B = \sqrt{\hbar/eB}$ and cyclotron frequency $\omega_c = \sqrt{2}v_F/\ell_B$ the Hamiltonian at the K point of the j-th layer ($j = 1, 2$) is transformed to a Landau level (LL) basis

$$h_{K,j} = -i\omega_c \begin{pmatrix} 0 & ae^{-i\theta_j} \\ -a^\dagger e^{i\theta_j} & 0 \end{pmatrix} \tag{4}$$

where $a^\dagger = (-2\partial_{\bar{z}} + z/2)/\sqrt{2}$ is the Landau level raising operator and θ_j is the rotation angle of the j-th layer. At the K' point $h_{K',j} = \sigma_y h_{K,j} \sigma_y$. Since the interlayer coupling matrices in Eqns. (2) and (3) are *local* in the layer-projected coordinates the bilayer LL Hamiltonian is

$$\mathcal{H}^{\text{SE}}_{KK} = \begin{pmatrix} h_{K,1} & \mathcal{V}\exp(i\varphi\sigma_z) \\ \mathcal{V}\exp(-i\varphi\sigma_z) & h_{K,2} \end{pmatrix} \tag{5}$$

for SE bilayers and in the SO case

$$\mathcal{H}^{\text{SO}}_{KK'} = \begin{pmatrix} h_{K,1} & \mathcal{V}(1+\sigma_z)/2 \\ \mathcal{V}(1+\sigma_z)/2 & h_{K',2} \end{pmatrix}. \tag{6}$$

Particle-hole symmetry allows the spectrum to be studied by squaring $\mathcal{H}$, yielding for SE bilayers

$$\left(\mathcal{H}^{\text{SE}}_{KK}\right)^2 = \begin{pmatrix} \omega_c^2(a^\dagger a + 1) + \mathcal{V}^2 & 0 & 0 & -i\omega_c\mathcal{V}(ae^{-i\alpha_1} + ae^{-i\alpha_2}) \\ 0 & \omega_c^2 a^\dagger a + \mathcal{V}^2 & i\omega_c\mathcal{V}(a^\dagger e^{i\alpha_1} + a^\dagger e^{i\alpha_2}) & 0 \\ 0 & -i\omega_c\mathcal{V}(ae^{-i\alpha_1} + ae^{-i\alpha_2}) & \omega_c^2(a^\dagger a + 1) + \mathcal{V}^2 & 0 \\ i\omega_c\mathcal{V}(a^\dagger e^{i\alpha_1} + a^\dagger e^{i\alpha_2}) & 0 & 0 & \omega_c^2 a^\dagger a + \mathcal{V}^2 \end{pmatrix} \tag{7}$$

where $\alpha_1 = \theta_1 + \varphi$ and $\alpha_2 = \theta_2 - \varphi$ and for SO bilayers

$$\left(\mathcal{H}^{\text{SO}}_{KK'}\right)^2 = \begin{pmatrix} \omega_c^2(a^\dagger a + 1) + \mathcal{V}^2 & 0 & 0 & -i\omega_c\mathcal{V}a^\dagger e^{i\theta_2} \\ 0 & \omega_c^2 a^\dagger a & i\omega_c\mathcal{V}a^\dagger e^{i\theta_1} & 0 \\ 0 & -i\omega_c\mathcal{V}ae^{-i\theta_1} & \omega_c^2 a^\dagger a + \mathcal{V}^2 & 0 \\ i\omega_c\mathcal{V}ae^{-i\theta_2} & 0 & 0 & \omega_c^2(a^\dagger a + 1) \end{pmatrix} \tag{8}$$

along with their valley reversed partners. Eqns. (7) and (8) demonstrate that for either family of structures the

Hamiltonian is block diagonal in a particular layer- and valley-polarized Landau level basis. For SE structures the interlayer coupling scatters states from LL_n in one layer only into states from $\mathrm{LL}_{\pm n}$ in the same valley of the neighboring layer, while in the SO structure LL_n in valley K of layer 1 couple only to $\mathrm{LL}_{\pm(n-1)}$ in valley K' of layer 2. Within these subspaces the Hamiltonians (7) and (8) can be diagonalized yielding

$$\varepsilon^{\mathrm{SE}}_{n,\kappa,\nu} = \pm\sqrt{n\omega_c^2 + \mathcal{V}^2 + \kappa\mathcal{V}\sqrt{2n\omega_c^2(1+\cos\varphi)}} \qquad (9)$$

and

$$\varepsilon^{\mathrm{SO}}_{n,\kappa,\nu} = \pm\sqrt{\frac{(2n+1)\omega_c^2 + \mathcal{V}^2 + \kappa\sqrt{\omega_c^4 + 2(2n+1)\omega_c^2\mathcal{V}^2 + \mathcal{V}^4}}{2}}, \qquad (10)$$

with valley ($\nu = \pm 1$) and branch ($\kappa = \pm 1$) indices, setting $\hbar = 1$. The eigenstates of the SE structures come in valley-degenerate pairs. SO structures have degenerate pairs of states along with a quartet of orbital states at $\varepsilon = 0$ (with indices $n = 0$, $\kappa = -1$, and $\nu = \pm 1$).

Figure 1 shows the evolution of the LL spectra as a function of B. For SE structures, the states disperse $\propto \sqrt{B}$ away from two coherence-split Dirac nodes and evolve at high field into two groups of branches that disperse away from the charge neutrality level. For SO structures the fermions are massive in both the low energy (around $E = 0$) and high energy (around $E = \pm\mathcal{V}$) branches and the LL's disperse linearly in B when $\omega_c \ll \mathcal{V}$ crossing over to the expected the $\sqrt{B}$ dependence in high field. For Bernal stacking $\mathcal{V} \gg \omega_c$ at experimentally realizable fields and one can eliminate the high energy bands giving an effective two band model for the "weak field" limit of the SO spectra [2]. By contrast in twisted SE and SO structures the coherence scale is small and all the degrees of freedom are accessible.

A striking prediction of Eqns. (9) and (10) is that the overlapping branches of Landau levels produce an amplitude modulation in the density of states. When $\varepsilon \gg \mathcal{V}$ for SE structures and $\varepsilon \gg (\mathcal{V}, \omega_c^2/\mathcal{V})$ for SO structures one can approximate $\varepsilon \approx \pm(\sqrt{n} + \kappa\beta\mathcal{V})$ where for (SE,SO) bilayers $\beta = (\cos(\varphi/2), 1/2)$. The density of states is enhanced whenever the energy of LL_n in one branch ($\kappa = -1$) overlaps the energy of LL_{n-m} in the other ($\kappa = 1$). This occurs for $m = 4\beta\mathcal{V}\sqrt{n}/\omega_c$ when $n \gg m$, and produces a beating pattern with period $\Delta E = \omega_c^2/4\beta\mathcal{V}$, most evident when $\Delta E \gg \omega_c \gg \mathcal{V}$. Superposition of the spectra produces a "Dirac comb."

Scanning tunneling spectroscopy (STS) [21] in modest magnetic fields can access these quantum oscillations in the single layer-projected density of states ρ_1 and thereby quantify the interlayer coherence. Theoretically, ρ_1 is studied conveniently by integrating out the second layer [22] generating an effective Hamiltonian for the first (exposed) layer $H_1^{\mathrm{eff}}(E) = H_1 + H_{\mathrm{int}}\left(E - H_2\right)^{-1} H_{\mathrm{int}}^{\dagger}$ with an energy-dependent self energy that is evaluated in each invariant subspace of Eqns. (5) and (6). The density of states is then obtained by a trace over the sublattice degrees of freedom and invariant subspaces: $\rho_1(E) = \sum_{n,\nu} \mathrm{Im\,tr}\left[E - i\gamma - H^{\mathrm{eff}}_{1,n,\nu}(E - i\gamma)\right]^{-1}$ with level broadening γ. Importantly, in both SE and SO structures the zero mode of the surface-projected problem occupies a special one dimensional subspace with

$$H^{\mathrm{eff,SE}}_{1,n=0} = |\mathcal{V}|^2/E;\ H^{\mathrm{eff,SO}}_{1,n=0,\nu} = \delta_{\nu,-1}E|\mathcal{V}|^2/(E^2 - \omega_c^2). \qquad (11)$$

Eqn. (11) demonstrates that the zero modes of each layer are always coherence-split by $2\mathcal{V}$ in SE bilayers but remain *exactly decoupled* for all SO bilayers.

These features can be seen clearly in the densities of states in Figures (2) and (3). The coherence splitting of the zero modes for SE bilayers and their degeneracy for SO is a fundamental signature of their different sublattice symmetries. At higher energy (Fig. (3)) quantum oscillations are clearly seen for both families. Although the $B = 0$ dispersions are nearly the *same* for these two structures at energies $E \gg \mathcal{V}$ (Fig. 1) the amplitude modulations near $E \simeq \omega_c^2/\beta\mathcal{V}$ are phase shifted, also reflecting their distinct low energy mass structure.

The modulations reflect the atomic registry in the bilayer and are most pronounced for short period superlattices. They are observable for $B > \mathcal{V}^2/2e\hbar v_F^2$, which requires a field scale of only 0.1 T for $\mathcal{V} \sim 10$ meV. For small fault angles the coherence scale $\mathcal{V}$ collapses, the magnetic field scale is correspondingly reduced and measurements will ultimately be limited by the finite quasiparticle lifetime. Interestingly, the modulation period $\Delta E = \hbar^2\omega_c^2/4\beta\mathcal{V} = \hbar eB/M^*$ describes the cyclotron frequency of a *massive* particle with $M^* \sim 3.5 \times 10^{-3} m_{\mathrm{e}}$ when $\mathcal{V} = 10$ meV. This can be understood from the semiclassical quantization of phase space orbits within the annulus bounded by the two coherence-split bands.

Remarkably, these oscillations should be most easily seen in the weak field regime when the layers are weakly coupled. For $\mathcal{V} < 0.5$ meV as suggested by microscopic calculations [16], the modulation period $\Delta E \sim$

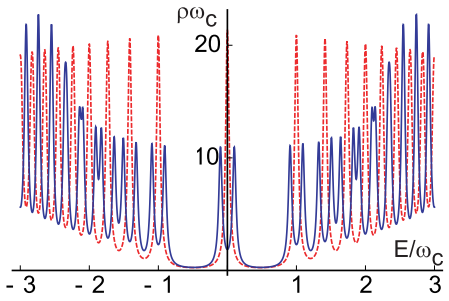

FIG. 2: Layer projected density of states for SE (blue) and SO(dashed red) twisted bilayers as a function of E/ω_c ($\hbar = 1$). Data are plotted for $\mathcal{V}/\omega_c = 0.1$, $\gamma = .03 \times \omega_c$ and $\varphi = \pi/4$. The low field states of the SO bilayer are weakly coherence split for the SE bilayer.

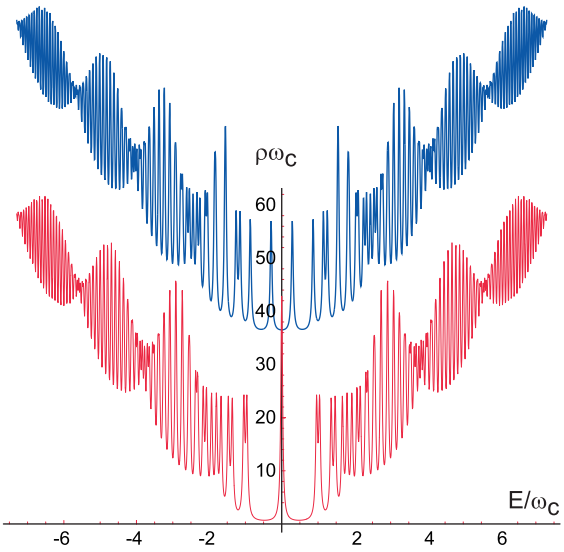

FIG. 3: Layer projected density of states as a function of E/ω_c over a wide energy range showing the amplitude modulation in the Dirac comb. Data are plotted for $\mathcal{V}/\omega_c = 0.3$ and $\varphi = 2\pi/3$. Top panel(blue, vertically offset) is for an SE bilayer and the lower panel (red) is for an SO bilayer.

$\hbar v_F^2 B/\mathcal{V} > 0.1\,\mathrm{eV}$ for $B = 0.1\,\mathrm{T}$. This is much larger than the Landau level spacing so the interference generates a smooth amplitude modulation extending over many quantized levels as shown in Fig. 3. The dependence of $\mathcal{V}$ on the rotation angle is unknown, but observation of these quantum oscillations can experimentally quantify this coherence scale.

These low field quantum oscillations are physically distinct from the Landau level structure studied for twisted graphene bilayers in high fields [23, 24]. Low angle faults offset the Dirac nodes at the zone corners K in neighboring layers introducing an energy scale $\Delta E = \hbar v_F K \sin(\theta/2)$ at which layer-decoupled Dirac cones intersect. Interlayer mixing of these states creates a saddle point singularity where the topology of the bands changes; in a magnetic field this is identified by an onset of enhanced coherence-splittings of nearly layer-degenerate LL states. For a rotation angle $\sim 1^\circ$, $\Delta E \sim 100\,\mathrm{meV}$ so for the n-th Landau level this occurs for $nB \sim 10\,\mathrm{T}$. Likewise the physics of the Dirac comb is distinct from the Hofstadter physics that arises when the magnetic length becomes commensurate with a superlattice translation, requiring $B \sim 4\,\mathrm{T}$ for $\theta \sim 1^\circ$ [25].

In summary we have studied the Dirac comb in the weak field Landau quantized spectra for twisted graphene bilayers: an interference phenomenon yielding an amplitude modulation of the LL spectra. This is important for low energy magnetotransport and provides an experimental probe of the interlayer coherence scale and its low energy mass structure.

This work was supported by the Department of Energy, Office of Basic Energy Sciences under contract DE-FG02-ER45118 (EJM) and by the NSF DMR-0820382 (MK).

* Electronic address: mele@physics.upenn.edu

[1] H. Min, A.H. MacDonald, Phys. Rev. B **77**, 155416 (2008).
[2] E. McCann and V.I. Fal'ko, Phys. Rev. Lett **96**, 086805 (2006).
[3] T. Ohta *et al.*, Science **313**, 951 (2006).
[4] E.V. Castro *et al.* Phys. Rev. Lett. **99**, 216802 (2007).
[5] Z. Li *et al.*, Phys. Rev. Lett. **102**, 037403 (2009).
[6] K.S. Novoselov *et al.*, Nature **438**, 197 (2004).
[7] Y. Zhang *et al.*, Nature **438**, 201 (2004).
[8] C. Berger *et al.*, Science **312**, 1191 (2006).
[9] J. Hass *et al.*, Phys. Rev. Lett. **100**, 125504 (2008).
[10] G. Li, A. Luican and E.Y. Andrei, Phys. Rev. Lett. **102**, 176804 (2009).
[11] M. Sprinkle *et al.* Phys. Rev. Lett. **103**, 226803 (2009).
[12] J. Hicks *et al.*, Phys. Rev. B **83**, 205403 (2011).
[13] A. Luican *et al.*, Phys. Rev. Lett. **106**, 126802 (2011).
[14] J.M.B. Lopes dos Santos, N.M.R. Peres, A.H. Castro Neto, Phys. Rev. Lett. **99**, 256802 (2007).
[15] S. Latil *et al.*, Phys. Rev. B **76**, 201402(R) (2007).
[16] S. Shallcross, S. Sharma and O.A. Pankratov, Phys. Rev. Lett.**101**, 056803 (2008).
[17] G. T. de Laissardière *et al.* Nano Lett. **10**, 804 (2010).
[18] E. J. Mele, Physical Review B **81**, 161405 (2010).
[19] R.Bistritzer and A.H. MacDonald, Phys. Rev. B **81** 245412 (2010); Proc. Nat. Acad. Sci. **108**,12233 (2011).
[20] D.P. DiVincenzo and E.J. Mele, Phys. Rev. B **29**, 1685 (1984).
[21] D.L. Miller *et al.* Science **324**, 924 (2009).
[22] M. Kindermann and P.N. First, Physical Review B **83**, 045425 (2010).
[23] R. de Gail *et al.*, arXiv:1103.3172.
[24] M-Y Choi, H-Y Hyun and Y. Kim, arXiv:1105.4551v1.
[25] R. Bistritzer and A.H. MacDonald, Phys. Rev. B **84**, 035440 (2011).